

Optimal Energy Storage System Control in a Smart Grid including Renewable Generation Units

A. Andreotti, G. Carpinelli and F. Mottola

Department of Electrical Engineering
University Federico II of Naples
Via Claudio, 21 I – 80125 Napoli (Italy)

Fax number: +39 081 2396897, e-mail: amedeo.andreotti@unina.it, guido.carpinelli@unina.it, fmottola@unina.it

Abstract. The paper deals with energy storage systems applications in Smart Grids. Several services can be performed thanks to the energy storage systems use, with objectives aimed at meeting needs internal or external to the Smart Grid. Optimal nonlinear constrained problems can be formulated and properly solved in order to perform the services in the best economical and technical way. In this paper, optimal control strategies are proposed in order to allow the Smart Grid to minimize internal losses and to sell energy and ancillary services during high power prices periods. The procedure involves the formulation of optimal power flow problems; proper objective functions and constraints are imposed to satisfying the services that have to be carried out. A numerical application on a 30-bus low voltage Smart Grid shows the effectiveness of the proposed procedure.

Key words

Smart Grid, Energy Storage Systems, Renewable Energies, Control strategies, Optimization techniques.

1. Introduction

Smart Grid means complex power networks that use bi-directional communications among Distributed Energy Resources (DERs), customers and a Central Control System (CCS), in order to optimize the power supply while guarantying the overall system efficiency. Use of a Smart Grid usually refers to power quality improvements, optimal exploitation of renewable energy resources, network self-repairing when failures happen, opportunity for the customers to manage their electricity usage for minimizing their expenses and so on [1-3].

On the other hand, liberalization of the power market and widespread use of DERs, in particular Dispersed Generation (DG) and Energy Storage Systems (ESSs), could enable Smart Grids to have a significant influence on electricity market prices and ancillary services [4]. As focused in [4], the charge/discharge of various ESSs can be controlled in order to guarantying proper applications. Further, in modern power distribution systems, where a significant amount of the total electricity demand is met by renewable generation, ESSs can mitigate the uncertainties of energy sources (such as solar and wind) and can store

the energy during high renewable production and/or low price periods, and deliver when either necessary or convenient. Based on the ESSs technologies, in [4] the applications of ESSs are classified in instantaneous, short-, mid- and long-term. Instantaneous and short-term applications are involved in real time regulations, for example aiming at ancillary services provision or integration of electric drive vehicles batteries in the networks [5, 6].

In the most general case, ESSs in a Smart Grid including renewable energies can operate with several objectives, aimed at meeting needs internal (for example, the minimization of losses) or external to the Smart Grid (for example, sell of energy during high power prices periods and storage of energy during the other periods). These objectives can be obtained thanks to a proper control of ESSs.

The problem of ESSs control in distribution systems with DG have been already treated in the relevant literature, (e.g. [7-10]). In [7], an ESS control algorithm, aimed at reducing the power exchange between the grid and the interconnected network, is proposed. In [8] a single-objective optimization problem is proposed for providing a ESS control strategy aimed at obtaining peak load shaving. Based on dynamic programming, the algorithm maximizes the benefit obtained by the peak shaving application. In [9] a methodology for operation of ESSs in distribution networks with wind generation is proposed. Through the formulation of a single-objective optimization problem, the algorithm aims at scheduling the ESSs daily active power provision, while minimizing the grid power losses. In [10] a methodology for emulating the distribution network behavior in presence of ESSs and DG is proposed. The algorithm is based on a single-objective optimization problem aimed at maximizing the profit provided by the power exchanged between ESSs and the grid.

The methodologies proposed in [7-10], such as other proposals, are based on the control of ESSs active power and their stored energy status but do not consider their potential to provide reactive power (thanks to the presence of interfacing static converters) for power losses reduction and voltage regulation. Moreover, they deal with either internal service (e.g. power losses or peak shaving) or external service (e.g. reducing the power

exchange between the grid and the interconnected network).

In this paper an optimal ESSs control strategy, based on both active and reactive hourly scheduling, is presented. The strategy is aimed at the optimal operation of Smart Grids for providing internal and external services simultaneously, unlike those already proposed in literature. More in detail, the paper formulates a single-objective optimization problem whose objective function is power losses minimization (internal service) while satisfying constraints on active and reactive power at the interconnection bus (external service).

The paper is organized as follows: in Section 2 the optimization problem is formulated, Section 3 reports a numerical application, and some conclusions are drawn in the final part of the paper.

2. The Optimization Problem

Let us consider a Low Voltage (LV) Smart Grid derived from an interconnection bus, and characterized by the presence of DG units and ESSs; a centralised control system is provided to implement proper procedures for the optimal grid operation. Some DG units and all the ESSs are connected through power electronic interfaces. The interconnection bus can be a Medium Voltage (MV) bus (in this case, a MV/LV transformer is present) or a LV bus (the Smart Grid is interconnected with a LV distribution network). Several services can be performed and optimal nonlinear constrained problems can be coherently formulated to perform the stated services in the best economical and technical way.

In this paper, a single objective-optimization problem is formulated in order to minimize Smart Grid losses (internal service), and make active or reactive power available to the interconnected network when it is required (external service). This kind of operation needs a proper ESSs control strategy aimed at coordinating their charging/discharging cycles during each day.

As an example, let us consider the qualitative daily load variation of Fig. 1; a strategy aimed at making available active power to the interconnected network during the hours of assumed high energy price (e.g. from 5:00 up to 22:00, in Fig. 1), would let the ESSs charge during the assumed hours of low energy price (e.g. from 22:00 up to 5:00, in Fig. 1). In this case, the ESS control strategy includes two operation stages: the first is the *charging cycle* performed during the low energy price hours and the second is the *discharging cycle* performed during the high energy price hours¹.

The strategy to be performed can be based on a typical Optimal Power Flow (OPF) that minimizes an objective function f_{obj} while meeting proper equality and inequality constraints, i.e.:

$$\min f_{obj}(\mathbf{X}, \mathbf{C}) \quad (1)$$

subject to

$$\psi(\mathbf{X}, \mathbf{C}) = 0, \quad (2)$$

$$\eta(\mathbf{X}, \mathbf{C}) \leq 0, \quad (3)$$

¹ For sake of simplicity, only two operation cycles are considered, however, a higher number of charging/discharging cycles can be easily considered.

where \mathbf{X} is the system state vector (voltage at all system busbars) and \mathbf{C} is the control vector. The procedure is applied for each control interval (for example, one hour or less) of the day. Depending on whether the control interval refers to the charging or to the discharging cycle, the input data, output data and optimization procedure are different.

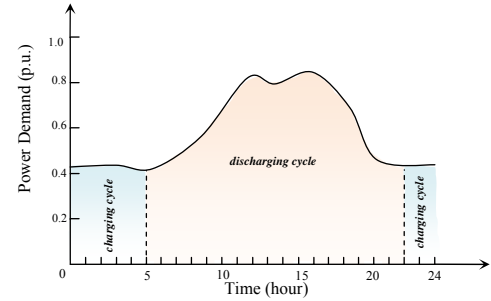


Fig. 1. Typical daily load variation.

A. Charging Cycle

During the j^{th} control interval of the charging cycle, problem *input variables* are the values of the initial energy stored in the ESSs that are outputs of the $j^{\text{th}}-1$ control interval (or outputs of the last interval of the discharging cycle in case of $j^{\text{th}}=1^{\text{st}}$), and both the forecasted loads power demand and forecasted DG units power production, for all the time intervals starting from the j^{th} control interval up to the end of the charging cycle. Problem *output variables* are the energy stored in the ESSs at the end of the j^{th} control interval that are inputs for the $j^{\text{th}}+1$ control interval (or inputs of the first interval of the discharging cycle in case j^{th} is the last of the charging cycle), the ESSs active powers, the DG units and ESSs reactive powers that have to be provided.

The *objective function* to be minimized is:

$$f_{obj}^j = \sum_{i \in \Omega_j} P_{losses,i} \quad (4)$$

where $P_{losses,i}$ is the Smart Grid power losses at the i^{th} time interval into the set Ω_j , which is the set of all the time intervals starting from the j^{th} control interval up to the end of the charging cycle.

The *equality constraints* are the typical power flow equations, properly formulated to take into account the problem variables. We note that the reactive power produced by the DG units and the active and reactive powers of the ESSs are control variables and, hence, are included into the power flow equations. We note also that the power flow equations have to be simultaneously solved for all the time intervals of the set Ω_j , i.e. from the j^{th} control interval up to the end of the cycle. In fact, a further equality constraint has to be included with reference to the energy stored in the ESSs that, at the end of the charging cycle, must have a specified value. In particular, for each ESS, the following constraint has to be satisfied:

$$E_{ESS,h,j_0} + \sum_{i \in \Omega_j} (P_{ESS,h,i} \Delta T_i) = E_{ESS,h}^{sp} \quad (5)$$

where E_{ESS,h,j_0} is the energy stored in the ESS located at node h at the begin of the j^{th} control interval (output of the $j^{\text{th}}-1$ control interval), $P_{ESS,h,i}$ is the charging power of the ESS located at node h in the i^{th} time interval in the set

Ω_j , ΔT_i is the corresponding duration, and $E_{ESS,h}^{sp}$ is the specified value of energy that has to be stored in the ESS located at node h at the end of the charging cycle.

The *inequality constraints* have to be satisfied for all the time intervals of the set Ω_j ; in particular:

- the voltage at all the busbars have to fall into an admissible range $[V_{min}, V_{max}]$, that is

$$V_{min} \leq V_{h,i} \leq V_{max} \quad h = 1, \dots, N \quad \forall i \in \Omega_j, \quad (6)$$

where N is the number of busbars;

- the active and reactive powers flowing through the interconnection bus are limited by the MV/LV transformer rate S_t (if present), that is

$$\sqrt{P_{1,i}^2 + Q_{1,i}^2} \leq S_t \quad \forall i \in \Omega_j, \quad (7)$$

where $P_{1,i}$ and $Q_{1,i}$ are the active and reactive powers through the interconnection bus during the i^{th} time interval in Ω_j ;

- line currents have to satisfy proper ratings, that is

$$I_{l,i} \leq I_{l,max}, \quad \forall l \in \Omega_L, \quad \forall i \in \Omega_j, \quad (8)$$

where $I_{l,i}$ and $I_{l,max}$ are the current of line l at the i^{th} time interval in Ω_j and its rating, respectively, and Ω_L is the set of network lines;

- ESSs active powers have to fall into an admissible range²:

$$|P_{ESS,h,i}| \leq P_{ESS,h,rate} \quad \forall i \in \Omega_j, \quad (9)$$

where $P_{ESS,h,rate}$ is the rating of the ESS located at node h ;

- ESSs stored energy have to fall into an admissible range:

$$E_{ESS,h,min} \leq E_{ESS,h,i} \leq E_{ESS,h,rate}, \quad \forall i \in \Omega_j, \quad (10)$$

where $E_{ESS,h,min}$ is the minimum value of the energy that has to be stored in the ESS located at node h (e.g., due to the depth of discharge) and $E_{ESS,h,rate}$ is the energy rate of the ESS located at node h ;

- ESSs and DG active and reactive powers are limited by the interfacing converters sizes, that is

$$\sqrt{P_{ESS,h,i}^2 + Q_{ESS,h,i}^2} \leq S_{ESS,h} \quad \forall i \in \Omega_j, \quad (11)$$

$$\sqrt{P_{DG,k,i}^2 + Q_{DG,k,i}^2} \leq S_{DG,k} \quad \forall i \in \Omega_j, \quad (12)$$

where $Q_{ESS,h,i}$ is the reactive power of the ESS located at node h during the i^{th} time interval, $P_{DG,k,i}$, $Q_{DG,k,i}$ are the active and reactive powers of the DG unit located at node k during the i^{th} time interval, $S_{ESS,h}$ and $S_{DG,k}$ are the sizes of the converters interfacing the ESS located at node h and the DG unit located at node k .

B. Discharging Cycle

During the n^{th} control interval of the discharging cycle, the problem *input variables* are the values of the initial energy stored in the ESSs that are outputs of the $n^{th}-1$ control interval (or outputs of the last interval of the charging cycle in case of $n^{th}=1^{st}$), the forecasted values of loads power demand and DG units power production, for the n^{th} control interval.

Problem *output variables* are the ESSs powers, the ESSs stored energy level at the end of the control interval that are inputs for the $n^{th}+1$ control interval (or inputs of the first interval of the charging cycle in case n^{th} is the last of the discharging cycle), the DG units and ESSs reactive

² For sake of simplicity, the constraints related to the efficiency are neglected. To take into account these constraints see [10].

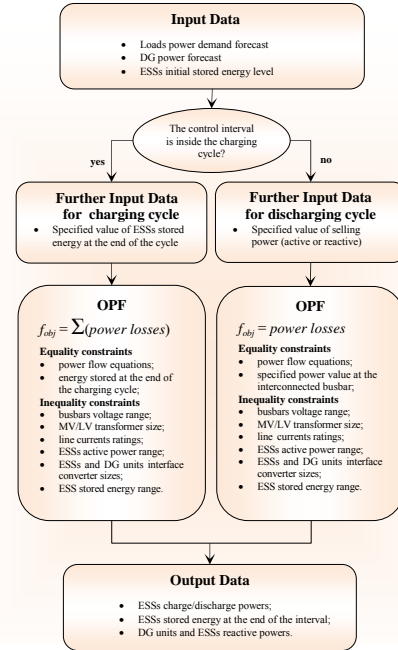


Fig. 2. Flow chart of the proposed procedure at the generic control interval.

powers that have to be provided during the n^{th} control interval.

Then, the *objective function* to be minimized is:

$$f_{obj}^n = P_{losses,n}, \quad (13)$$

where $P_{losses,n}$ is the Smart Grid power losses at the n^{th} control interval.

The *equality constraints* are, once again, the typical power flow equations, properly formulated to take into account the problem variables (also in this case the reactive power produced by the DG and the active and reactive powers of the ESSs are included into the power flow equations). Note also that, in the discharging cycle, power flow equations have to be solved only for the n^{th} current control interval.

An *equality constraint* has also to be included with reference to the active power that has to be guaranteed at the interconnection bus. For the n^{th} control interval, the following equality constraint is then imposed³:

$$P_{1,n} = P_n^{sp}, \quad (14)$$

where $P_{1,n}$ is the active power at fundamental frequency through the interconnection bus during the n^{th} control interval and P_n^{sp} is its specified value. A similar constraint can be imposed with reference to the reactive power at the interconnection bus, if required.

With reference to the *inequality constraints*, relations from (6) to (12) have to be satisfied only with reference to the n^{th} control interval.

Eventually, in Fig. 2 the flow chart of the whole proposed control procedure is shown. We note that the forecasting for the control intervals can be effected by applying a Bayesian-based approach such as that proposed in [11]. In addition, we note that the solution of the formulated optimal problem can be used as inputs of the real time control of the network shown in [6].

³ During the operation of a Smart Grid, it could happen that the energy stored in ESSs is not sufficient to satisfy (14); to face with this problem, and to obtain a feasible solution, this constraint could be neglected and the difference $(P_{1,n} - P_n^{sp})$ properly added to the objective function (13).

3. Numerical application

The proposed procedure was applied to the 30-busbar LV balanced 3-phase Smart Grid shown in Fig. 3. Line parameters and loads nominal power are those reported in [12] and [6], respectively. The LV network is connected to a MV network through a 20/0.4 kV, 250 kVA transformer with $v_{cc}\%=4.2\%$. The Smart Grid includes two photovoltaic (PV) and one wind turbine (WT) DG units and four ESSs. The PV units (10 kW and 20 kW peak power) are located at busbars #15 and #9 respectively, and are connected through DC/AC converters. The WT unit, equipped with a 7.5 kW asynchronous generator, is located at bus #24. The ESSs (a 10 kW unit located at bus #19 and three 5 kW units located at busbars #12, #6 and #30, respectively) are REDOX battery units, with 4 hours charging time, and are connected to the Smart Grid through DC/AC converters. ESSs siting and sizing were chosen applying the approach proposed in [13]. The control time interval is assumed to be equal to one hour.

Three case studies are considered: the first case (*Case A*) refers to an hour of the charging cycle (from 22:00 up to 5:00); the second case (*Case B*) refers to an hour of the discharging cycle (from 5:00 up to 22:00), where a value of 4 kW of active power was assumed to be guaranteed at the interconnection bus; the third case (*Case C*) refers to the same hour of the *case B* but with a value of 1 kVAr of reactive power that has to be guaranteed at the interconnection bus. In all the simulations, a constant value of 1.05 p.u. is considered for the voltage at the MV busbar of the transformer (node #1 in Fig. 3).

A. Case A

The input data are the forecasted load demands and DG power productions at 22.00 (the considered hour). It is assumed that the ESSs are 5% charged, due to their behaviour in the previous hours. As an example, Fig. 4 shows the assumed load demand forecast at bus #4, expressed in p.u. of the rated load powers. Fig. 5 shows the assumed WT power production forecast. Obviously, during the period under study, the PV production is assumed to be zero. Table I shows the ESSs active and reactive powers obtained applying the proposed approach.

Table I. – ESSs powers at 22:00

ESSs node	Active power (kW)	Reactive power (kVAr)
19	-10.00	6.63
12	-5.00	1.98
6	-5.00	2.01
30	-5.00	1.70

As further examples of the obtained results, Figs. 6 show the charging profiles of the ESSs located at busbars #19 (Fig. 6.a) and #12 (Fig. 6.b); Figs. 7 show the reactive power profiles of the ESSs located at busbars #19 (Fig. 7.a) and #12 (Fig. 7.b); their stored energies are shown in Fig. 8.a (ESS at #19) and Fig. 8.b (ESS at #12). Finally, Fig. 9 shows the network voltage profile; for comparative purposes, in the same figure, the profile without the ESSs is also reported. This last profile is obtained by solving the power flow equations without the injection of active and reactive powers by the ESSs (note that active and reactive powers injected by the PV units are equal to zero in both cases).

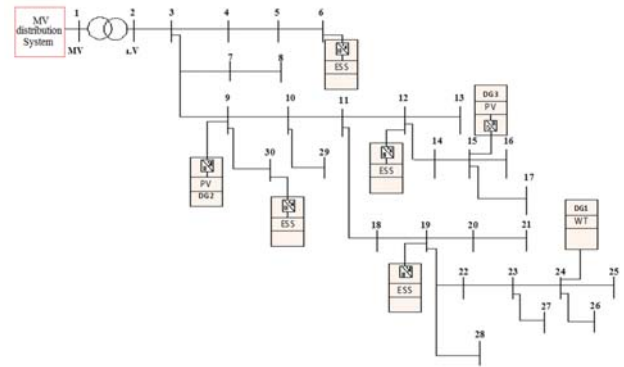


Fig. 3. LV Smart Grid test system.

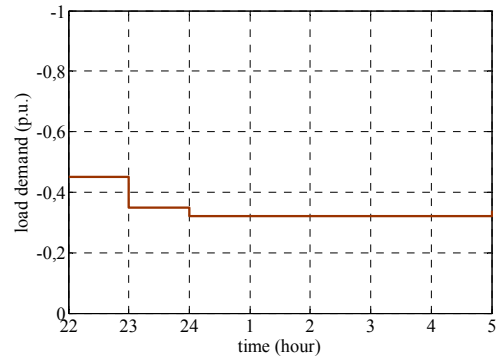


Fig. 4. Load demand forecast at 22:00.

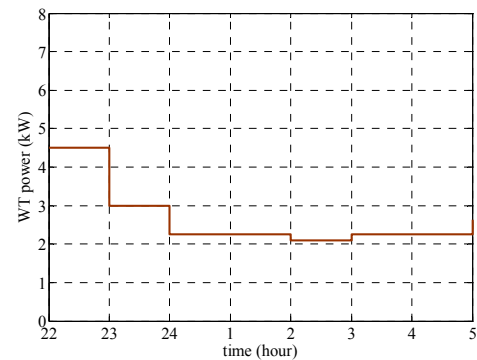


Fig. 5. WT production forecast at 22:00.

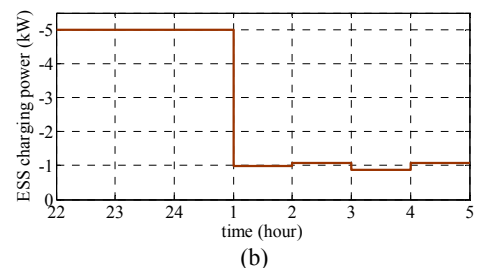
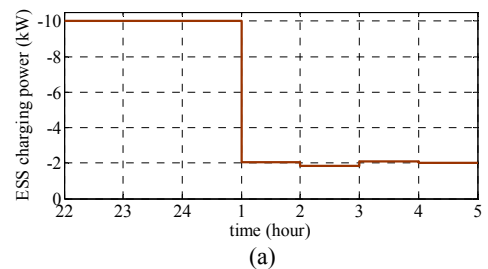


Fig. 6. ESS charging profile at bus #19 (a) and at bus #12 (b), calculated at 22:00.

Figs. 6 show how the proposed strategy makes it possible to charge the ESSs mainly during high wind production periods.

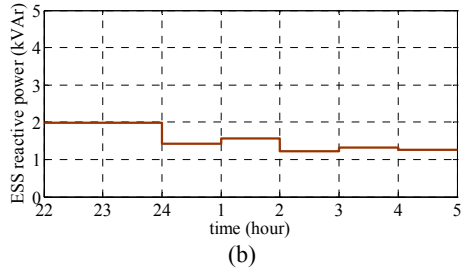
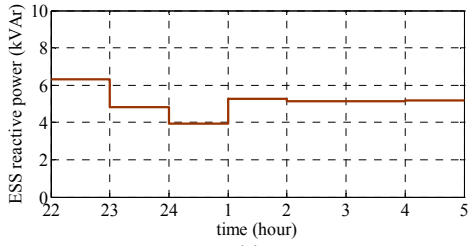


Fig. 7. ESS reactive power at bus #19 (a) and at bus #12 (b), calculated at 22:00.

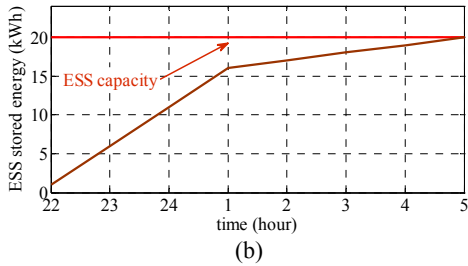
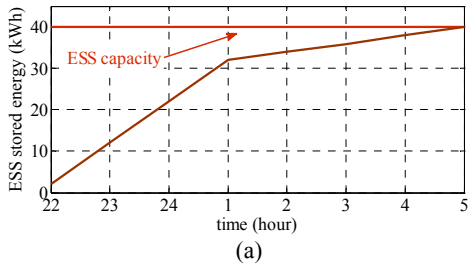


Fig. 8. ESS stored energy profile at bus #19 (a) and at bus #12 (b), calculated at 22:00.

Figs. 7 show the ESSs contribution to the voltage regulation by the injection of reactive power. Figs. 8 show that the solution satisfies the constraint related to the ESSs full charging. In Fig. 9 it appears, as expected, that the presence of ESSs determines a voltage profile lower than that obtained without the use of ESSs. Anyway, the proposed control strategy makes it possible to satisfy the voltage constraints.

B. Case B

As far as the *case B*, the procedure was applied at a generic hour of the discharging cycle (15:00). The assumed load demand forecast is 86% of the rated load power. The assumed WT and PV power production forecast are shown in Table II; the ESSs are 40% charged, due to their behaviour in the previous hours.

Table II. – DG production forecast at 15:00

DG type	node	Active Power (kW)
WT	24	6.00
PV	15	10.00
PV	9	20.00

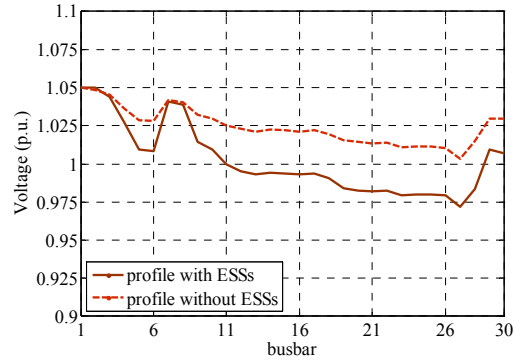


Fig. 9. Voltage profile calculated at 22:00 with and without ESSs active and reactive powers (*case A*).

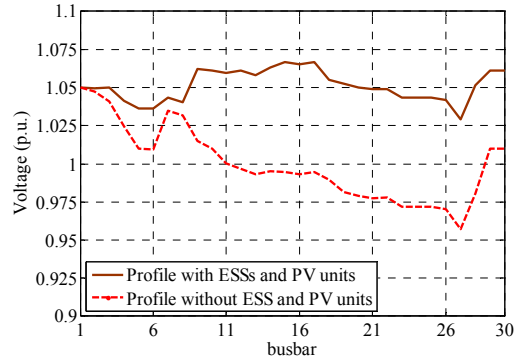


Fig. 10. Voltage profile calculated at 15:00 with and without active and reactive powers of ESSs and PV units (*case B*).

Table III shows the obtained active and reactive powers of the PV units and ESSs. From the results reported in Table III, it is interesting to highlight the significant contributions of all devices in terms of reactive power provision, in order to guarantee both the voltage limits and losses minimization. In fact, unlike *case A*, power production of PV units is not zero and PV reactive power provision is controlled by the procedure.

Table III. – PV and ESS powers (*case B*)

Unit	node	Active Power (kW)	Reactive Power (kVAr)
ESS	19	9.26	7.64
ESS	12	0.34	5.04
ESS	6	5.00	3.32
ESS	30	3.57	1.91
PV	15	10.00 ^(*)	1.35
PV	9	20.00 ^(*)	4.04

^(*) This is an input data (the same of Tab. II).

Fig. 10 shows the corresponding network voltage profile; for comparative purposes, in the figure the profile without ESSs and PV units is also reported. This profile is obtained by solving power flow equations without the injection of active and reactive powers by the ESSs and PV units. In Fig. 10 it is shown that the presence of ESSs in the discharging stage, causes a voltage profile higher than that obtained without ESSs and PV units. Anyway, the control strategy makes it possible to satisfy the voltage constraints. It should be noted that the reactive power imported from the interconnection bus is 3.76 kVAr.

C. Case C

As far as the *case C*, the procedure was applied to the same hour of *case B* and, then, the same input data were assumed. Table IV shows the obtained reactive power of PV units and the active and reactive powers of ESSs. From Table IV, it is interesting to evidence the significant contributions of all devices in terms of reactive power, in order to guarantee also the voltage limits and the losses minimization.

Table IV. – PV and ESS powers (*Case C*)

Unit	node	Active Power (kW)	Reactive Power (kVAr)
ESS	19	2.74	11.68
ESS	12	1.04	3.34
ESS	6	1.00	4.92
ESS	30	1.36	2.22
PV	15	10.00 ^(*)	1.14
PV	9	20.00 ^(*)	4.78

^(*) This is an input data (the same of Tab. II).

Fig. 11 shows the corresponding network voltage profile; for comparative purposes, in the same figure, the profile without ESSs and PV units is also reported.

Fig. 11 clearly shows that also in *case C*, the voltage constraints are satisfied. Finally, it should be noted that the active power imported from the interconnection bus is 8.19 kW.

4. Conclusions

In this paper ESSs operation strategies have been discussed for Smart Grids applications. In particular, optimal control strategies have been proposed in order to allow the Smart Grid to minimize internal losses and sell energy and ancillary services during high power price periods. The procedures involves the formulation of optimal power flows, with proper objective functions; proper constraints are imposed to satisfy the services that have to be performed. A numerical application to a 30-bus low voltage Smart Grid has shown the effectiveness of the proposed procedure and the feasibility of the results.

Future researches will consider further improvements to reduce the computational efforts of the proposed procedure.

Acknowledgement

This paper is funded in the framework of the agreement of the MSE – CNR Program for Triennial Plan of the System Research and Annual Operational Plan for Research and Development Activities of general interest for the National Electrical System (Electrical Storage Systems).

References

[1] E. Santacana, G. Rackliffe, Le Tang and Xiaoming Feng, "Getting Smart", Power and Energy Magazine, IEEE, Vol. 8, No. 2, March-April 2010, pp.41-48.

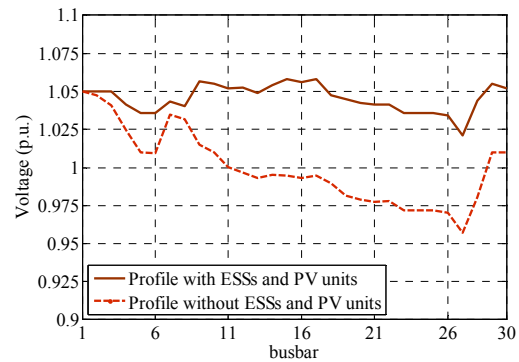


Fig. 11. Voltage profile calculated at 15.00 with and without active and reactive powers of ESSs and PV units (*case C*).

[2] K. Moslehi and R. Kumar, "A Reliability Perspective of the Smart Grid", Smart Grid, IEEE Transactions on, Vol.1, No.1, June 2010, pp. 57-64.

[3] A. Ipakchi and F. Albuyeh, "Grid of the future", Power and Energy Magazine, IEEE, Vol.7, No.2, March-April 2009, pp.52-62.

[4] K.C. Divya, J. Østergaard, "Battery energy storage technology for power systems: An overview", Electric Power System Research, Vol. 79, 2009, pp. 511-520.

[5] W. Kempton, J. Tomic: "Vehicle-to-grid power fundamentals: Calculating capacity and net revenue", Journal of Power Sources, Vol. 144, Issue 1, June 2005, pp. 268-279.

[6] A. Bracale, P. Caramia and D. Proto, "Optimal Operation of Smart Grids Including Distributed Generation Units and Plug in Vehicles", accepted for International Conference on Renewable Energies and Power Quality (ICREPQ'11), April 13-15, 2011, Las Palmas de Gran Canaria (Spain).

[7] U. Kwhannet, N. Sinsuphun, U. Leeton and T. Kulworawanichpong, "Impact of energy storage in micro-grid systems with DGs", Power System Technology (POWERCON), 2010 International Conference on, 24-28 October 2010, pp. 1-6.

[8] A. Oudalov, R. Cherkaoui and A. Beguin, "Sizing and Optimal Operation of Battery Energy Storage System for Peak Shaving Application", Power Tech, 2007 IEEE Lausanne, 1-5 July 2007, pp.621-625.

[9] C. Abbey and G. Joos, "Coordination of Distributed Storage with Wind Energy in a Rural Distribution System", 42nd IEEE Industrial Applications Annual Meeting, 23-27 September 2007, pp.1087-1092.

[10] F. Geth, J. Tant, E. Haesen, J. Driesen and R. Belmans, "Integration of energy storage in distribution grids", Power and Energy Society General Meeting, 2010 IEEE, 25-29, July 2010, pp. 1-6.

[11] A. Bracale, G. Carpinelli, D. Proto, A. Russo and P. Varilone, "New Approaches for Very Short-term Steady-State Analysis of An Electrical Distribution System with Wind Farms", Special Issue "Wind Energy", Energies, 2010, 3, pp. 650-670.

[12] R. Angelino, A. Bracale, M. Mangoni and D. Proto: "Centralized Control of Dispersed Generators Providing Ancillary Services in Distribution Networks Part II: Numerical Applications", in Proc. IEEE/PES 44th International Universities' Power Engineering Conference (UPEC) 2009, September 1-4, 2009, Glasgow (GB).

[13] G. Carpinelli, F. Mottola, D. Proto and A. Russo, "Optimal Allocation of Dispersed Generators, Capacitors and Distributed Energy Storage Systems in Distribution Networks", in Proc. IEEE Modern Electric Power Systems 2010, September 20-22, Wroclaw (PL).